Journal of Photochemistry and Photobiology A: Chemistry 208 (2009) 164–170

Contents lists available at ScienceDirect

Journal of Photochemistry and Photobiology A: Chemistry

journal homepage: www.elsevier.com/locate/jphotochem

On the structure and excited electronic state lifetimes of cytidine self-assemblies with extended hydrogen-bonding networks

Nina K. Schwalb[1], Friedrich Temps*

Institut für Physikalische Chemie, Christian-Albrechts-Universität zu Kiel, Olshausenstr. 40, D-24098 Kiel, Germany

ARTICLE INFO

Article history:
Received 3 June 2009
Received in revised form 10 August 2009
Accepted 10 September 2009
Available online 23 September 2009

Keywords:
Cytidine
DNA base pairs
Hydrogen bonding
Self-assembly
Fluorescence
Electronic relaxation
Radiationless transitions

ABSTRACT

The nucleoside cytidine (C) assembles in extended hydrogen-bonded aggregates in neat apolar solvents like *n*-hexane, when carrying inert hydrophobic groups at the 2′,3′,5′-oxygen atoms of the ribose moiety. The ensuing structures, which constitute model systems for DNA super-structures such as triplexes or quadruplexes, were elucidated by FTIR spectroscopy and further characterized by UV spectroscopy. The lifetimes of the optically excited electronic states of the aggregates were investigated using femtosecond UV fluorescence up-conversion spectroscopy. Time profiles were measured after excitation at a number of pump wavelengths between 296 nm $\geq \lambda_{pump} \geq$ 262 nm. The bi-exponential decay curves were characterized by time constants (with 2σ error limits) of $\tau_{1,C} = 0.58(1)$ ps (88–95% fractional amplitudes) and $\tau_{2,C} = 19.4(13)$ ps (12–5%) independent of the pump wavelength. The results indicate that the C multimers compared to the monomer do not gain photostability by coupled excited-state electron–proton transfer in the H-bonded networks, in contrast with recent findings for G·G and the G·C Watson–Crick dimer.

1. Introduction

The structure and shape of DNA is not limited to a single, unique double helix form, but can show variations depending on the base sequence and on external factors. It is well known, for example, that there are several duplex structures (e.g., A- or Z-type DNA) next to the normal B-type double helix differing in diameter, helical repeat, and twist angle [1,2]. In addition, sequences that are rich in homopurine and homopyrimidine repeats can form DNA super-structures like triplexes or quadruplexes [3–5]. The latter arise from guanine-rich sequences in eukaryotic centromeres and telomeres, which play decisive roles for cellular senescence, growth arrest, and apoptosis [5]. In DNA triplexes, a third oligonucleotide strand binds to the purines of the Watson–Crick (WC) pairs of a double helix in a (reverse-)Hoogsteen pattern, leading to the so-called H-DNA motif [6]. Furthermore, the so-called i-motif DNA arises by the association of two duplexes with tracts of hemi-protonated cytosine–cytosine base pairs [7,8]. It is believed that the highly specific recognition of a target duplex sequence may cause site-specific alterations and site-directed mutagenesis [6,9]. On the other hand, the precise recognition of a target duplex on triplex formation offers therapeutic potential, and information on the involved hydrogen-bonding (H-bond) networks is therefore of substantial interest in drug design [6,10–12].

Recent direct time-resolved experimental investigations of the ultrafast electronic deactivation dynamics of isolated H-bonded DNA base pairs in solution revealed that the guanosine–cytidine (G·C) WC pair displays a strongly reduced fluorescence lifetime of the optically excited state compared to C or G on their own [13,14]. The H-bonds between the complementary strands in a G·C-containing double helix may also contribute to the photodynamics and stability of duplex DNA [15]. As homopurine and homopyrimidine pairs appear in DNA super-structures like tri- and quadruplexes, where they form extended H-bonded networks, we became interested in the so far unknown photophysical and photochemical properties of such larger aggregates.

In this paper, we present a study on the formation of model systems for DNA tri- and quadruplexes formed from self-assembled cytidine in solution in dry neat *n*-hexane (*n*-C_6H_{14}) and, in particular, an investigation of the excited electronic state lifetimes of the ensuing complexes. The structures of different aggregates of cytidine with extended H-bonding networks are shown in Fig. 1.

The H-bonded cytidine complexes are obtained in neat nonpolar solvents by employing a derivative of the nucleoside carrying *tert*-butyldimethylsilyl (TBDMS) groups at the 2′,3′,5′-O atoms of the ribose. The bulky organic protecting groups enhance the solubilities of the molecules in aprotic organic solvents, where the formation of

* Corresponding author.
E-mail address: temps@phc.uni-kiel.de (F. Temps).
URL: http://www.uni-kiel.de/phc/temps (F. Temps).
[1] Present address: Bayer Technology Services GmbH, D-51368 Leverkusen, Germany.

1010-6030/$ – see front matter © 2009 Elsevier B.V. All rights reserved.
doi:10.1016/j.jphotochem.2009.09.011

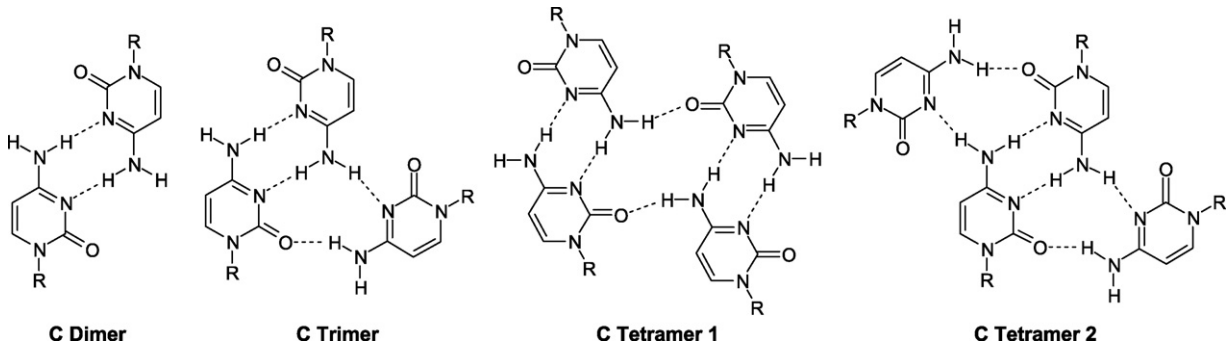

Fig. 1. Structures of the H-bonded dimer, a trimer, and two tetramers of C. Several of these motifs can arrange to larger super-structures. Tetramer 1, for instance, which is made up of two dimers, can form long tapes by adding further dimers to the left and right.

H-bonds between the bases is strongly enforced [16–21]. The ensuing association depends on solvent and is much more extensive in n-C_6H_{14} than in other solvents (e.g., $CHCl_3$) studied before [18,19]. The structures of the aggregates in n-C_6H_{14} were investigated by FTIR and by static UV absorption and fluorescence spectroscopies. Moreover, the excited electronic state decay dynamics were probed by femtosecond UV fluorescence spectroscopy. The lifetimes of the optically excited states of the measured H-bonded multimers turned out to be longer than for the cytidine monomer in H_2O and other H-bonded nucleoside dimers investigated recently in $CHCl_3$ [13,14]. The study lays out the path for forthcoming research on mixed DNA triplex motifs, such as G·G·C, and other super-structures.

2. Experimental section

2′,3′,5′-O-TBDMS-protected cytidine and 3′,5′-O-TBDMS-protected 2′-deoxycytidine (denoted in the following as $C(TBDMS)_3$ resp. $dC(TBDMS)_2$, or simply as C and dC when obvious from the context) were synthesized based on the protocol of Ogilvie [22] and purified by flash column chromatography. The products were checked by NMR spectroscopy and no traces of impurities were found.

The formation of H-bonded aggregates of C was monitored at room temperature as function of concentration by FTIR spectroscopy on a Bruker IFS 66v spectrometer at a resolution of 0.25 cm^{-1} in a variable pathlength cuvette with CaF_2 windows. Measurements were carried out in n-C_6H_{14} (Uvasol purity, Merck) at initial concentrations between 0.2 mM $\leq c_0 \leq$ mM. The well soluble C derivative was employed, because the dC derivative was easily soluble only in $CHCl_3$, and only to a small extent in CCl_4, but little in n-C_6H_{14}. The H-bonded complexes in $CHCl_3$ and in CCl_4 (>99 resp. 99.9% purity, Sigma–Aldrich) were investigated as function of concentration using dC. However, control spectra of C taken in $CHCl_3$ and in CCl_4 at a single c_0 were practically identical with reference spectra of dC in these solvents (except for the higher intensities of the bands associated with the larger number of TBDMS groups).

UV absorption measurements were performed as function of concentration and temperature on a Shimadzu UV-2401 desktop spectrometer. In addition, static fluorescence spectra were measured on a Horiba Jobin-Yvon Fluoromax 4 spectrometer to check for band shifts on aggregation, especially around λ_{fl} = 350 nm, where the emission was monitored in the time-resolved experiment. The excitation wavelengths were the same as in the subsequent femtosecond measurements. As the sample concentrations were too high for the standard 90° detection geometry, the fluorescence spectra were recorded in reflection by placing the cuvette at ≈45° to avoid inner filtering effects and ensure a linear response. Measurements at 90° and at 45° of the monophosphates at different concentrations in water verified that the band shapes were reproduced correctly.

Time-resolved fluorescence measurements were performed on C in n-C_6H_{14} solution using the up-conversion setup described in some detail previously [23]. The tunable fs UV excitation pulses were supplied by a Ti:Sa-pumped non-collinear optical parametric amplifier (NOPA) with a frequency doubling stage and focused into the sample cell (1 mm optical pathlength) with the polarization at the magic angle. The resulting fluorescence was refocused into a BBO crystal for non-collinear type I sum frequency generation (SFG) with time-delayed gate pulses (100 μJ) from the Ti:Sa pump laser by two 90° off-axis parabolic mirrors. The SFG light was monitored by a single-photon counter at λ_{SFG} = 241 nm (fluorescence wavelength λ_{fl} = 350 nm) through a f = 0.1 m double monochromator.

All fluorescence-time profiles were measured at two sample concentrations (c_0 = 0.1 and 1.0 mM) to check for possible changes in the aggregation. Each set of experiments consisted of up to four repeated scans to ensure reproducibility and one scan of the neat solvent to rule out unwanted background signals. The sample solutions were continuously pumped through the cell to avoid accumulation of photoproducts between two laser shots. Moreover, the excitation pulse energies were reduced to ≤50 nJ per pulse, and the allocated liquid volumes in the sample reservoir were at least 100–250 mL to avoid potential contaminations by photodamaged products. Measurements in ethanol, in which both plain and TBDMS-protected C are well soluble, verified that the TBDMS groups do not affect the excited electronic state lifetimes of the nucleosides [14].

The recorded fluorescence-time profiles were analyzed using a nonlinear least-squares fitting routine based on the Levenberg–Marquardt algorithm implemented in MATHEMATICA software [24]. Fits were performed on single profiles and globally with model functions consisting of a sum of decaying exponentials convoluted with a Gaussian for the instrument response function (IRF).

3. Results

3.1. FTIR spectra

Fig. 2 displays the measured FTIR spectra of cytidine and its H-bonded aggregates in the region of the NH stretch vibrations, which are involved in the H-bonding networks, between ω = 3200 and 3600 cm^{-1}. The different panels show the effective absorption coefficients $\epsilon_{eff} = \log(I_0/I)/(c_0 d)$ at a series of concentrations for (a) dC in $CHCl_3$, (b) dC in CCl_4, and (c) C in n-C_6H_{14}. In addition, Fig. 3 compares the spectra for C in $CHCl_3$, CCl_4, and n-C_6H_{14} on a single plot at about c_0 = 1.6 mM.

The FTIR spectra at low concentrations in $CHCl_3$ (Fig. 2a) display intense vibrational bands which clearly belong to the asymmetric

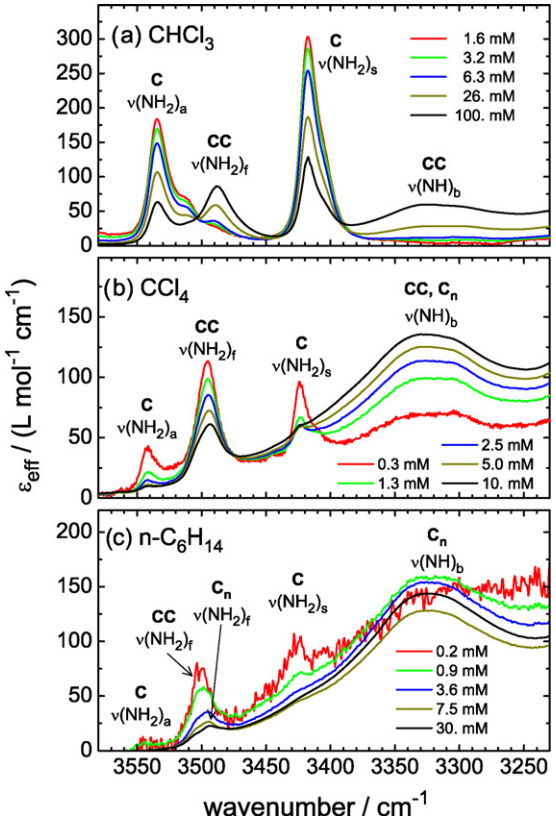

Fig. 2. FTIR spectra of (a) dC(TBDMS)$_2$ in $CHCl_3$, (b) dC(TBDMS)$_2$ in CCl_4, and (c) C(TBDMS)$_3$ in n-C_6H_{14} at different concentrations. The labels assign the observed features to vibrations of the monomer (C), dimer (CC), and larger aggregates (C_n).

and symmetric N–H stretch vibrations $\nu(NH_2)_a$ and $\nu(NH_2)_s$ of the C monomer at $\omega = 3534$ and 3417 cm^{-1} [18]. The free N–H stretch vibration $\nu(NH_2)_f$ at 3488 cm^{-1} of the NH_2 involved in the dimer formation grows in with increasing c_0. The broad absorptions below 3450 cm^{-1} are typical for H-bonded nucleobase complexes. The structure of the dimer that is present in $CHCl_3$ is depicted in Fig. 1. The experimental frequencies are in good agreement with quantum chemical calculations for the C monomer and the C·C dimer [21].

The vibrational spectra in CCl_4 (Fig. 2b) demonstrate a much stronger aggregation than in $CHCl_3$. The frequencies of $\nu(NH_2)_a$ and $\nu(NH_2)_s$ shift to 3541 and 3424 cm^{-1}, respectively, and $\nu(NH_2)_f$ moves to 3496 cm^{-1}. The concentration dependence shows, however, a rapid decrease of the monomer bands and the dimer band

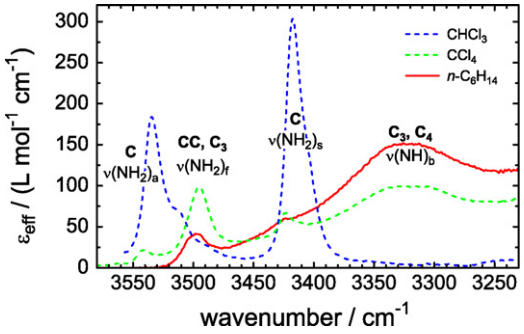

Fig. 3. Comparison of the FTIR spectra of C(TBDMS)$_3$ in $CHCl_3$, CCl_4, and n-C_6H_{14} at a concentration of $c_0 = 1.6$ mM. The monomer and dimer bands in n-C_6H_{14} have practically disappeared already at concentrations below 1 mM. The broad absorptions below 3450 cm^{-1} are typical for H-bonded complexes. The region below 3200 cm^{-1} was inaccessible due to the strong absorptions by the n-C_6H_{14}.

with increasing c_0, suggesting aggregation to larger complexes (trimers, tetramers). The monomer is clearly visible only in the spectrum at $c_0 = 0.3$ mM. The $\nu(NH_2)_f$ band of the dimer can be followed up to $c_0 = 10$ mM, but its intensity decreases with increasing c_0 as well. As can be seen from Fig. 3, the spectrum in CCl_4 appears to take an intermediate position between those in $CHCl_3$ and n-C_6H_{14}.

The measured spectra of C in n-C_6H_{14} (Fig. 2c) differ very drastically from those in $CHCl_3$, and continue the trends seen in CCl_4 (cf. Fig. 3). Monomer vibrations are very weakly visible at $\omega = 3545$ and 3424 cm^{-1} only at the lowest concentrations (see the spectrum at $c_0 = 0.2$ mM), but vanish rapidly with increasing c_0. The same is true for the dimer band of $\nu(NH_2)_f$ at $\omega = 3499$ cm^{-1}, which also decreases immediately with higher c_0. At the same time, there is a small red-shift to $\omega = 3493$ cm^{-1}. Those spectral positions are typical for a free N–H stretch vibration of an NH_2 group with its other N–H in an H-bond, but such NH_2 groups seem to be rare for C in n-C_6H_{14}. From the pronounced spectral changes, we therefore have to conclude that the measured vibrational spectra of C in n-C_6H_{14} stem predominantly from larger H-bonded multimers rather than dimers. The outstanding spectral signatures of those multimers are the virtual absence of the $\nu(NH_2)_f$ band, the intense broad absorption at $\omega \approx 3300$–3340 cm^{-1}, and several overlapping broad, intense bands in the $\omega \approx 3070$–3200 cm^{-1} region. The latter are hidden under the strong solvent absorptions in n-C_6H_{14}, but were observable in CCl_4. Thus, the spectra are consistent with the formation of triads or tetrads as sketched in Fig. 1. Trimer formation might occur by binding of an additional C monomer to a symmetric C·C dimer, tetramer structures can either be formed from two dimer subunits (tetramer 1) or from a dimer binding two monomers on opposite sides (tetramer 2). Calculated bond energies per monomer unit are all quite similar [21], and it appears impossible at this stage to distinguish between those complexes. Considering the structures in Fig. 1, and the virtual absence of $\nu(NH_2)_f$ bands in the vibrational spectra, it is indeed likely that the trimers and tetramers form even larger H-bonded aggregates. Tetramer 1, in particular, may form long tapes, which may become predominant at higher concentrations. All larger structures imply the formation of N–H···O=C bonds. As this H-bond to a carbonyl group may be slightly stronger compared to the N–H···N motif in the C·C dimer, the shift of $\nu(NH_2)_f$ by ≈6 cm^{-1} from 3499 cm^{-1} in the C·C dimer to 3493 cm^{-1} in the multimers appears reasonable. The CO stretch/NH_2 bend region of the spectra of C unfortunately show a only a strongly overlapped broad band without analyzable signature, which does not help further.

3.2. Static UV absorption and fluorescence spectra

The static UV absorption and fluorescence spectra of C in n-C_6H_{14} are displayed in Fig. 4a and b. The spectral shape of the absorption is rather similar to C in $CHCl_3$ and unprotected cytidine in H_2O. The experimental absorption maxima are at $\lambda_{abs}^{max} = 278$ nm (n-C_6H_{14}), 281 nm ($CHCl_3$), and 271 nm (unprotected cytidine in H_2O). Thus, the absorptions in n-C_6H_{14} and $CHCl_3$ are red-shifted relative to unprotected cytidine in H_2O by 7 resp. 10 nm. Based on the dielectric constants, we would normally expect the red-shift with respect to isolated monomeric cytidine in vacuo to be largest in H_2O, smaller in $CHCl_3$, and slightly smaller again in n-C_6H_{14}. Interestingly, the spectrum of C in n-C_6H_{14} measured at $T = 65$ °C is almost identical with that in $CHCl_3$ at 25 °C (Fig. 4a). These different effects will be examined further in Section 4.

The static fluorescence spectra given in Fig. 4b were recorded after excitation at the absorption maximum to obtain a rough orientation on the range of emission wavelengths for the subsequent up-conversion measurements. The spectrum in n-C_6H_{14} appears slightly red-shifted from that in $CHCl_3$, which we attribute with some due caution to the presence of different emitting species

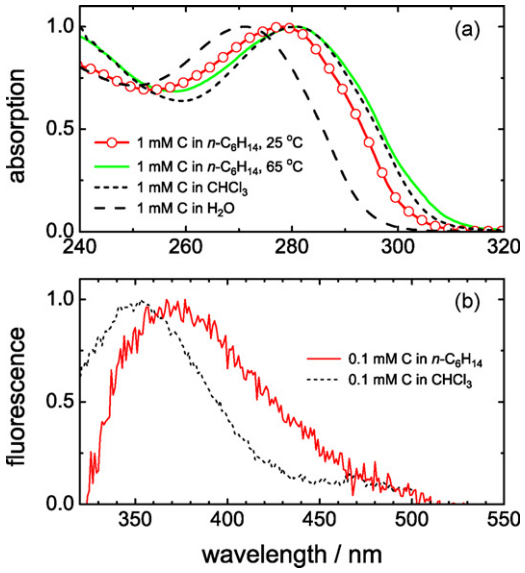

Fig. 4. (a) UV absorption spectra of C(TBDMS)$_3$ in n-C_6H_{14} and $CHCl_3$ and unprotected cytidine in H_2O. (b) Static fluorescence spectra of C(TBDMS)$_3$ in n-C_6H_{14} and $CHCl_3$. The very weak fluorescence spectra were normalized to their maxima for better comparison after subtraction of the background traces (scattered light and unavoidable minute impurities) by the solvents.

in the two solvents (monomers in $CHCl_3$, larger aggregates in n-C_6H_{14}). In both cases, however, the spectra were very weak due to the known low fluorescence quantum yield of C [25] and therefore hard to measure accurately, especially in the reflection mode which had to be used. Thus, spurious small other differences (e.g., on the low intensity red edge of the spectra) in Fig. 4b are due to background correction problems and should not be taken as significant.

3.3. Time-resolved fluorescence measurements

The fluorescence-time profiles of C(TBDMS)$_3$ in n-C_6H_{14} measured after excitation at λ_{pump} = 296, 290, 283, and 262 nm are displayed in Fig. 5. The detection wavelength of λ_{fl} = 350 nm is close to the maximum of the emission (Fig. 4b). The observed decay curves could be described using two exponentials with time constants (with error limits of last digits in parentheses) of

$\tau_{1,C}$ = 0.58(1) ps (95%),
$\tau_{2,C}$ = 19.4(13) ps (5%).

The quoted fractional amplitudes refer to the data at λ_{pump} = 262 nm. At longer pump wavelengths, the contribution of the slow component increased slightly (to 12% at λ_{pump} = 296 nm). Because of the low absorption of the excitation light by the sample close to the electronic origin, the data taken at λ_{pump} = 296 nm are somewhat noisier. Other than that, however, no significant dependences of the decay times on λ_{pump} or on c_0 were found.

4. Discussion

The present work employed a straighforward route for the preparation of H-bonded aggregates of the DNA base cytidine, which can now be studied in detail, e.g., as model systems for biologically important non-classical DNA super-structures like triplexes or quadruplexes. The applied experimental approach based on suitable O′-protected nucleoside derivatives in aprotic solvents is easily applicable to other natural or non-natural nucleobases. Using the same strategy, we already studied the excited electronic state fluorescence lifetimes of H-bonded dimers of C and G and the G·C WC pair in solution in $CHCl_3$ [13,14]. The resulting structures were elucidated so far mainly by FTIR spectroscopy, but additional methods (e.g., NMR spectroscopy) could be applied in principle as well.

4.1. FTIR spectra and structures of the H-bonded cytidine complexes

Using FTIR spectroscopy, we observed the formation of dimers of C (resp. dC) in solution in $CHCl_3$ and C trimers, tetramers, and/or larger aggregates in CCl_4 and, in particular, in n-C_6H_{14}. It is difficult to distinguish the structures of these larger multimers from the vibrational spectra alone owing to the extended H-bonding net-

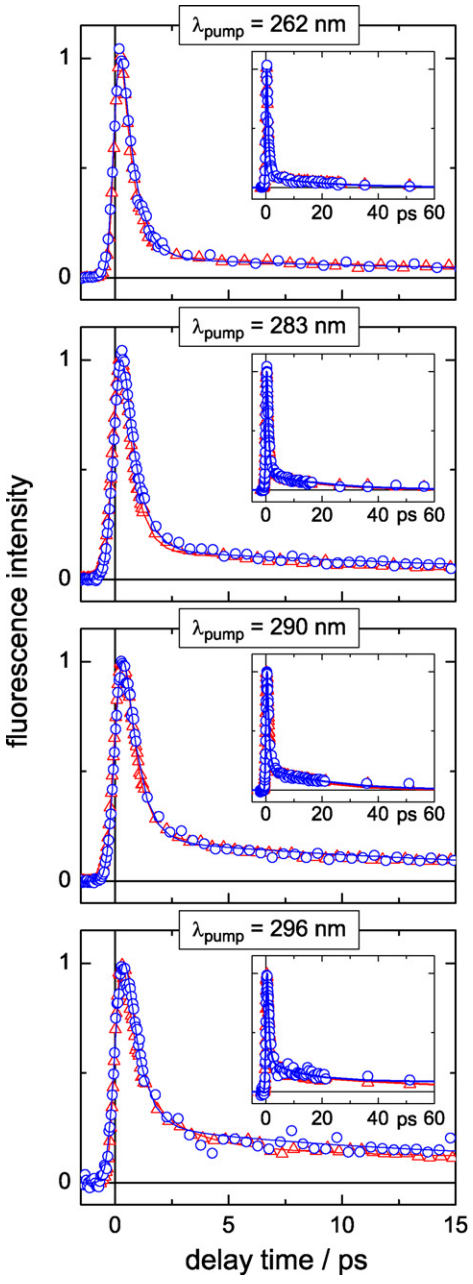

Fig. 5. Measured fluorescence decay profiles for the C aggregates in n-C_6H_{14} at the different excitation wavelengths. Open circles represent data points at c_0 = 0.1 mM, open triangles data points at c_0 = 1.0 mM, and solid lines are the fitted time profiles. The insets show the data and fits on the time scale up to Δt = 60 ps.

works (cf. Fig. 1), but this might be feasible in future work by NMR spectroscopy. Moreover, as C tetramer 1 on the one hand and C tetramer 2 or the C trimer on the other differ in their H-bonding networks (Fig. 1), two-dimensional IR spectroscopy [26–28] may offer the required means to unravel the complex structures.

4.2. UV spectra

The near UV absorption spectra of the C aggregates in *n*-C_6H_{14}, C (resp. dC) in $CHCl_3$, and unprotected free cytidine in water measured at room temperature resemble each other largely in shape, but the absorption maxima in $CHCl_3$ and *n*-C_6H_{14} are red-shifted by a few nm with respect to the cytidine in water. The red-shift in $CHCl_3$ is slightly larger than that in *n*-C_6H_{14}. The spectral shifts could arise, at least in principle, from a range of mechanisms, including bulk solvatochromic effects by the dielectric constant (ε) of the solvent, weak solute–solvent hydrogen-bonding interactions, influences of the H-bonds within the dimers and multimers on their electronic states, or exciton coupling [29–31] in even larger (e.g., stacked) aggregates of H-bonded dimers and multimers.

Investigations of solvent effects on the steady-state absorption and fluorescence spectra and the dynamics of the excited electronic states are reported in the literature for several uracil derivatives [32,33]. By the bulk effect, absorption spectra in solution are red-shifted with respect to the isolated molecules in the gas phase owing to dielectric stabilization of the excited state, when the excited state reached in the optical transition has a higher dipole moment than the ground state. Under these conditions, solvation thus decreases the energy gap between the highest occupied and lowest unoccupied molecular orbitals (HOMO and LUMO, respectively). Accordingly, the absorption maxima of the uracils appear more red-shifted in a series of alcohols with increasing dielectric constants [33]. Vice versa, the observed blue-shift in the present work on going from $CHCl_3$ ($\varepsilon = 4.8$, $\lambda_{abs}^{max} = 281$ nm) to the non-polar *n*-C_6H_{14} ($\varepsilon = 1.9$, $\lambda_{abs}^{max} = 278$ nm) is therefore in order. The absorption spectrum of cytidine in water with its maximum at $\lambda_{abs}^{max} = 271$ nm, i.e., at a shorter wavelength than for the TBDMS derivatives in $CHCl_3$ and in *n*-C_6H_{14} despite the much stronger polarity of water, seems to stand out in this respect. It has to be kept in mind in this discussion, however, that, although the electron systems in cytidine and TDBMS-protected cytidine should in principle be similar, the bulky hydrophobic organic groups modify the local environment of the cytidine chromophore and may therefore bias the comparisons between the unprotected and protected molecules in different solvents. A 10 nm red-shift also occurs, for example, on going from uracil to 1-cyclohexyluracil in water [32].

Theory has found it difficult to quantitatively predict the bulk solvent effect on the excited-state energies of cytosine in water [34]. However, the 0–0 transitions of two specific cytosine–H_2O structures were calculated to be blue-shifted by ≈0.25 eV (corresponding to ≈15 nm) with respect to free cytosine in the gas phase, owing to the reduced H-bonding capacities of the spectroscopically active excited $\pi\pi^*$ states of the monohydrates. This suggests a distinctive cytosine–H_2O H-bonding effect on the absorption spectrum in water as critical factor. We note further in this context that protonation of the chromophore as in 2′-deoxycytidine·HCl induces a red-shift to $\lambda_{abs}^{max} = 275$ nm (as well as a shortening of the excited electronic state lifetime measured by fs transient absorption spectroscopy [35]).

Solute-to-solvent H-bonding effects in $CHCl_3$ may not be completely negligible as well, but should be much weaker considering the low hydrogen-bond donor (HBD) activity for $CHCl_3$ of $\alpha = 0.20$ [36] on the Kamlet–Taft scale [37,38]. On this scale, $\alpha = 0$ for the aprotic *n*-C_6H_{14} versus, for example, $\alpha = 0.86$ and 1.12 for the protic solvents ethanol and acetic acid, respectively.

As noted, the C aggregates in *n*-C_6H_{14} exhibit a hypsochromic effect (blue-shift) with respect to the C species in $CHCl_3$. A shift in that direction goes in line with the bulk solvent effect. However, at the concentration of $c_0 = 1$ mM used, the FTIR spectra demonstrated extensive multimerization by H-bonding in *n*-C_6H_{14}, but the predominating presence of C monomers (i.e., little H-bonding between C units) in $CHCl_3$. On heating to 65 °C, where the aggregates partially dissociate, the absorption in *n*-C_6H_{14} is red-shifted by $\Delta\lambda = 3$ nm to $\lambda_{abs}^{max} = 281$ nm, i.e., we have a hypsochromic shift of the aggregates at room temperature with respect to less associated structures at elevated temperature. Such an effect is characteristic for exciton coupling in H-aggregates by stacking of the chromophores [31]. Exciton coupling is ubiquitous in the DNA double helix, where the dipole–dipole interactions between the chromophores in the well-organized nucleobase stacks held in place by the sugar–phosphate backbone lead to collective delocalized excited electronic states, which are manifest by blue-shifted near-UV absorption maxima [30,31]. Thus, one should examine the possibility for formation of "columnar" aggregates of the H-bonded structures in our case.

Columnar phases are indeed known for the monophosphates (GMP, dGMP) of guanosine and deoxyguanosine in water ([39] and references therein). G has the highest tendencies of the DNA bases to form such structures, but this happens at far higher concentrations than used in the present work. The experimentally measured GMP threshold concentrations in water for the formation of G quadruplexes and, beyond, columnar aggregates from GMP [39] are indeed roughly three orders of magnitude higher than the millimolar cytidine concentrations in our study. Moreover, GMP aggregation is inherently connected to the presence of alkali ions as templating agents for the G quadruplex motif. NMR measurements of various O′-protected deoxyguanosines in $CDCl_3$ at concentrations and other conditions similar to our experiments showed only H-bonding and no signs for stacked aggregates [40,41]; liquid crystalline phases were obtained only when the deoxyguanosines were dissolved in the required "minimal" amounts of hydrocarbons [41], i.e., orders of magnitude higher concentrations.

Cytidine is known to have a much lower ability for self-aggregation than guanosine. The pyrimidine bases in general lend themselves less to base stacking than the purine bases. Further, H-bonding energies between the nucleobases are higher than π-stacking bond energies [42,43] (albeit by a lesser amount than usually thought [43]). Thus, considering the absence of ionic species in our experiments (including the absence of protonated C as in the i-motif DNA), the employed orders of magnitude lower concentrations in *n*-C_6H_{14} (1.0 mM in the UV absorption measurements, 0.1–1.0 mM in the fs time-resolved experiments) compared to the conditions, under which the liquid cristalline phases of guanosine were observed, and the additional aspect that the TBDMS protecting groups of our cytidine derivative are loaded with methyl groups, which are naturally solvophilic towards *n*-C_6H_{14}, it is not likely (although it cannot be rigorously excluded) that our experimental observations arise mostly from other aggregates than H-bonded ones.

Summing up this paragraph with some caution, we state that the temperature dependent UV measurements suggest some dissociation of the C multimer network in *n*-C_6H_{14} to smaller aggregates on heating, but that more systematic studies of the ensuing solvents effects and the aggregation are desirable.

4.3. Fluorescence-time profiles

The lifetimes of the optically excited electronic states of the H-bonded C self-assemblies as revealed by time-resolved UV fluorescence measurements were in our main focus. The obtained

Table 1
Comparison of the measured fluorescence decay times of the H-bonded complexes of C with reported related excited-state lifetimes in the literature.

Compound or complex[a]	Solvent	τ_1 ps	a_1 %	τ_2 ps	a_2%
Cyt	Gas[b]	0.16	n/a[c]	1.9	n/a[c]
dC	H_2O[d]	0.40	100	...	...
C	H_2O[e]	0.70	n/a[c]	...	...
C	H_2O[f]	2.90	87	12.0	9
CMP	H_2O[g]	0.41	86	1.7	14
dC	H_2O[h]	0.63	n/a[c]	...	...
dC(TBDMS)$_2$	$CHCl_3$[i]	0.63	95	21.0	5
[dC(TBDMS)$_2$]$_2$	$CHCl_3$[j]	>1	...	...	...
[C(TBDMS)$_3$]$_n$	n-C_6H_{14}[k]	0.58	95	19.4	5
[G·C]	$CHCl_3$[l]	0.30	100	...	...

[a] All data following excitation around $\lambda_{pump} < 262$ nm.
[b] For cytosine in molecular beam [44].
[c] Not available.
[d] For deoxycytidine from single-exponential fit to fluorescence decay data [45].
[e] From transient absorption measurements on cytidine at $\lambda_{probe} = 340$ nm [46].
[f] From transient absorption measurements on cytidine at $\lambda_{probe} = 250$ nm [46].
[g] For CMP in buffered solution at pH 7 from fluorescence decay (this laboratory).
[h] For protonated Cyd$^+$ [35].
[i] For dC(TBDMS)$_2$ from fluorescence decay [14].
[j] For [dC(TBDMS)$_2$]$_2$ from fluorescence decay [14].
[k] This work.
[l] For TBDMS-protected G·C WC pair in $CHCl_3$ from fluorescence decay [13,14].

fluorescence decay times are compared with related experimental data in Table 1.

The observed lifetimes for the C multimers agree quite well with those obtained for monomeric C in $CHCl_3$. Likewise, the electronic relaxations of cytosine, cytidine, or CMP in H_2O show similar bi-exponential behavior and the measured decay constants are just a bit faster than in $CHCl_3$ or in n-C_6H_{14} [13,14,45,47]. This hints that the relative energies of the excited electronic states are not strongly affected by the aggregation and that the observed fluorescence should result from monomer-like rather than delocalized (excitonic) states. Only the C·C dimer [13,14] appears to lack the sub-picosecond decay component displayed by all other profiles and thus shows a slower relaxation of the optically excited electronic state(s).

Transient absorption measurements [46] and theoretical studies [48–53,34] on isolated DNA pyrimidine bases have revealed that the internal conversion to the electronic ground state (S_0) proceeds via at least two distinctive pathways. In the main channel, the wavepacket prepared in the spectroscopically bright $\pi\pi^*$ state evolves from its Franck–Condon (FC) region to S_0 by a direct conical intersection (CI). A secondary route involves at least one optically dark, long-lived $n\pi^*$ state, which is populated during the relaxation process via a three-fold degenerate CI. This leads to a bifurcation of the excited-state population and the observed excited-state dynamics becomes bi-exponential. The direct pathway is reflected by τ_1 and the secondary route through the dark $n\pi^*$ state by τ_2. The two nonradiative pathways are simultaneously active in the pyrimidines in a variety of solvent environments [32]. However, as one of the minimum energy pathways (MEP) in the monomer involves an out-of-plane bending motion of the NH_2 group, it is conceivable that this route can be slowed down by a higher energy barrier en route to the respective CI in the H-bonded dimer and the larger aggregates.

Gas phase data on cytosine are bi-exponential as well [54,44], but differ in quantitative detail from those in solution. The $n\pi^*$ state and the triplet population, which are not negligible in the pyrimidines [46], are not directly observable in the fluorescence up-conversion measurements.

The excited-state lifetime of protonated cytidine is similar to that of the neutral nucleoside [35]. Nevertheless, although protonation leaves the nucleobase isoelectronic, the red-shift of its UV absorption maximum by several nm indicates a change of the electronic structure. In contrast, [dC]$_{18}$ DNA strands in H_2O, which exist in a hemi-protonated form even at neutral pH, have prolonged excited-state lifetime, but it has been shown that these are induced by secondary structure [55].

5. Conclusions

The present paper reported on the formation and the photodynamics of H-bonded self-assemblies of cytidine in solution in n-hexane. The ensuing structures were elucidated from the changes in the N–H stretch vibrational spectra on concentration in different solvents. The UV absorption spectra of cytidine and its derivatives in different solvents exhibit some visible changes as well, but more systematic studies of the underlying solvents effects remain desirable.

From the performed time-resolved fluorescence measurements, it became evident that the radiationless electronic relaxation rates in the investigated C multimers do not seem to benefit from the formation of the extended H-bonding network(s). This agrees with results obtained for the C·C dimer, but it contrasts with the situation for H-bonded G·G aggregates and the G·C WC base pair [13,14]. The latter exhibit drastically shortened excited-state fluorescence lifetimes compared to the respective monomers, which has been attributed to ultrafast transitions from the optically prepared $\pi\pi^*$ excited state to a charge-transfer (CT) state followed by intermolecular proton transfer involving the G imino group [56,57]. Such a mechanismus apparently does not occur in cytidine self-aggregates. It seems quite plausible that the highly dipolar intermediate CT state is energetically inaccessible, especially in a nonpolar solvent like n-C_6H_{14}.

Adopting another point of view, the "non-natural" C multimers that were observed are of interest also because of the light they shed on the evident ability of C to form self-assemblies beyond the standard WC base pairing scheme. The G·G·C and C·G·C triads, which occur in triplex DNA, come to mind next. Here, a G-rich third strand attaches to G·C-rich runs of a normal duplex through reverse-Hoogsteen bonding to the G sites. Likewise, a C-rich third strand can bind to G·C runs through Hoogsteen pairing. Work on such mixed aggregates is underway.

Acknowledgments

The financial support of this work by the Deutsche Forschungsgemeinschaft and the Fonds der Chemischen Industrie is gratefully acknowledged. The authors also thank J. Gripp for syntheses of several batches of the TBDMS-protected cytidine.

References

[1] W. Saenger, Principles of Nucleic Acid Structure, Springer, New York, 1983.
[2] V.A. Bloomfield, D.M. Crothers, I. Tinoco, Nucleic Acids: Structures, Properties and Functions, University Science Books, Sausalito, 2000.
[3] M.D. Frank-Kamenetskii, S.M. Mirkin, Annu. Rev. Biochem. 64 (1995) 65.
[4] M. Mills, L. Lacroix, P.B. Arimondo, J.L. Leroy, J.C. Froncois, H. Klump, J.L. Mergny, Curr. Med. Chem. – Anti-Cancer Agents 2 (2002) 627.
[5] J.T. Davis, Angew. Chem. 116 (2004) 684.
[6] A. Jain, G. Wang, K.M. Vasquez, Biochimie 90 (2008) 1117.
[7] K. Gehring, J.L. Leroy, M. Guéron, Nature 363 (1993) 561.
[8] M. Guéron, J.L. Leroy, Curr. Opin. Struct. Biol. 10 (2000) 326.
[9] M. Duca, P. Vekhoff, K. Oussedik, L. Halby, P.B. Arimondo, Nucleic Acids Res. 36 (2008) 5123.
[10] P. Simon, F. Cannata, J.P. Concordet, C. Giovannangeli, Biochimie 90 (2008) 1109.
[11] S. Neidle, G.N. Parkinson, Biochimie 90 (2008) 1184.
[12] Y. Qin, L.H. Hurley, Biochimie 90 (2008) 1149.
[13] N.K. Schwalb, F. Temps, J. Am. Chem. Soc. 129 (2007) 9272.
[14] N.K. Schwalb, T. Michalak, F. Temps, J. Phys. Chem. B, submitted for publication.
[15] N.K. Schwalb, F. Temps, Science 322 (2008) 243.
[16] R.M. Hamlin, R.C. Lord, A. Rich, Science 148 (1965) 1734.
[17] Y. Kyogoku, R.C. Lord, A. Rich, Science 154 (1966) 518.

[18] Y. Kyogoku, R.C. Lord, A. Rich, Biochim. Biophys. Acta 179 (1969) 10.
[19] P. Carmona, M. Molina, A. Lasagabaster, R. Excobar, A.B. Altabef, J. Phys. Chem. 97 (1993) 9519.
[20] L. Biemann, T. Häber, D. Maydt, K. Schaper, K. Kleinermanns, J. Chem. Phys. 128 (2008) 195103.
[21] T. Michalak, N.K. Schwalb, J. Gripp and F. Temps, Spectrochim. Acta A, submitted for publication.
[22] K.K. Ogilvie, Can. J. Chem. 51 (1973) 3799.
[23] N.K. Schwalb, F. Temps, J. Phys. Chem. A 113 (2009), doi:10.1021/jp9021773.
[24] Mathematica Version 6.0 (Wolfram Research, Inc., 2007).
[25] P.R. Callis, Annu. Rev. Phys. Chem. 34 (1983) 329.
[26] A.T. Krummel, M.T. Zanni, J. Phys. Chem. B 110 (2006) 13991.
[27] J. Bredenbeck, J. Helbing, C. Kolano, P. Hamm, Chem. Phys. Chem. 8 (2007) 1747.
[28] L. Szyc, J.R. Dwyer, E.T.J. Nibbering, T. Elsaesser, Chem. Phys. 357 (2009) 36.
[29] S. Marguet, D. Markovitsi, P. Millié, H. Sigal, S. Kumar, J. Phys. Chem. B 102 (1998) 4697.
[30] B. Bouvier, T. Gustavsson, D. Markovitsi, P. Millié, Chem. Phys. 275 (2002) 75.
[31] E. Emanuele, D. Markovitsi, P. Millié, K. Zakrewska, Chem. Phys. Chem. 6 (2005) 1387.
[32] P.M. Hare, C.E. Crespo-Hernández, B. Kohler, J. Phys. Chem. B 110 (2006) 18641.
[33] T. Gustavsson, N. Sarkar, Á. Bányász, D. Markovitsi, R. Improta, Photochem. Photobiol. 83 (2007) 595–599.
[34] L. Blancafort, A. Migani, J. Photochem. Photobiol. A 190 (2007) 283.
[35] R.J. Malone, A.M. Miller, B. Kohler, Photochem. Photobiol. 77 (2003) 158.
[36] Y. Marcus, Chem. Soc. Rev. (1993) 409.
[37] M.J. Kamlet, R.W. Taft, J. Am. Chem. Soc. 98 (1976) 377.
[38] R.W. Taft, M.J. Kamlet, J. Am. Chem. Soc. 98 (1976) 2886.
[39] P. Mariani, F. Spinozzi, F. Federiconi, H. Amenitsch, L. Spindler, I. Drevensek-Olenik, J. Phys. Chem. B 113 (2009) 7934.
[40] J.L. Sessler, M. Sathiosathan, K. Doerr, V. Lynch, K.A. Abboud, Angew. Chem. Int. Ed. 39 (2000) 1300.
[41] G. Gottarelli, S. Masiero, E. Mezzina, G.P. Spada, P. Mariani, M. Recanatini, Helv. Chim. Acta 81 (1998) 2078.
[42] J. Sponer, J. Leszczynski, V. Vetter, P. Hobza, J. Biomol. Struct. Dyn. 13 (1996) 695.
[43] J. Cerny, P. Hobza, Phys. Chem. Chem. Phys. 9 (2007) 5291.
[44] C. Canuel, M. Mons, F. Piuzzi, B. Tardivel, I. Dimicoli, M. Elhaninea, J. Chem. Phys. 122 (2005) 074316.
[45] D. Onidas, D. Markovitsi, S. Marguet, T. Gustavsson, J. Phys. Chem. B 106 (2002) 11367.
[46] P.M. Hare, C.E. Crespo-Hernández, B. Kohler, Proc. Natl. Acad. Sci. U.S.A. 104 (2007) 435.
[47] C.E. Crespo-Hernández, B. Cohen, P.M. Hare, B. Kohler, Chem. Rev. 104 (2004) 1977.
[48] K. Tomi, J. Tatchen, C.M. Marian, J. Phys. Chem. A 109 (2005) 8410.
[49] M. Merchán, R. González-Luque, T. Climent, L. Serrano-Andrés, E. Rodrguez, M. Reguero, D. Peláez, J. Phys. Chem. B 110 (2006) 26471.
[50] K.A. Kistler, S. Matsika, J. Phys. Chem. A 111 (2007) 2650.
[51] K.A. Kistler, S. Matsika, J. Phys. Chem. A 111 (2007) 8708.
[52] K.A. Kistler, S. Matsika, J. Chem. Phys. 128 (2008) 215102.
[53] H.R. Hudock, T.J. Martinez, Chem. Phys. Chem. 9 (2008) 2486.
[54] S. Ullrich, T. Schulz, M.Z. Zgierski, A. Stolow, Phys. Chem. Chem. Phys. 6 (2004) 2796.
[55] B. Cohen, M.H. Larsen, B. Kohler, Chem. Phys. 350 (2008) 165.
[56] A.L. Sobolewski, W. Domcke, Phys. Chem. Chem. Phys. 6 (2004) 2763.
[57] A.L. Sobolewski, W. Domcke, C. Hättig, Proc. Natl. Acad. Sci. U.S.A. 102 (2005) 17903.